Soft Matter

Cite this: *Soft Matter*, 2012, **8**, 10100

www.rsc.org/softmatter

PAPER

Interactions of distinct quadrupolar nematic colloids

Z. Eskandari,[ac] N. M. Silvestre,*[ab] M. Tasinkevych*[de] and M. M. Telo da Gama[ab]

Received 2nd May 2012, Accepted 18th July 2012
DOI: 10.1039/c2sm26022k

The effective interaction between spherical colloids in nematic liquid crystals is investigated in the framework of the Landau-de Gennes theory. The colloids differ in their surface interaction with the nematic liquid crystal. The particles induce quadrupolar far-field distortions in the nematic matrix, favouring homeotropic and the other degenerate planar anchoring of the nematic director. In the strong anchoring regime the colloids with homeotropic anchoring are accompanied by an equatorial disclination line defect, known as "Saturn-ring", while the colloids with degenerate planar anchoring nucleate a pair of antipodal surface defects, called "boojums". In the linear (large-distance) regime, the colloidal interactions are of the quadrupolar type, with quadrupoles of opposite signs. These are attractive when the colloids are aligned either parallel or perpendicular to the far-field director. At short distances, non-linear effects including "direct" interactions between defects give rise to a repulsion between the particles, which prevents them from touching each other. This finding supports the stability of nematic colloidal square crystallites the assembly of which has been reported recently.

1 Introduction

The self-assembly of colloidal particles into structures with controlled spatial ordering is of great importance in colloid science, with particular interest in the assembly of photonic crystals[1] – artificially produced periodic dielectric structures designed to control and manipulate light. In this context, a variety of colloidal structures assembled in liquid crystal (LC) matrices,[2,3] combined with the unique mechanical and electro-optical properties of the LC host,[4] are promising candidates for the development of colloid crystals with tunable photonic properties.

In conventional colloids, in isotropic fluids, the colloidal particles interact *via* van der Waals, electrostatic, or steric forces. These forces are isotropic, and their range does not exceed a few tens of nanometers. In contrast, when dispersed in a LC, due to its long-range orientational molecular ordering, colloidal particles interact predominantly through long-range anisotropic forces.[5,6] The origin of these forces is the elastic distortion of the LC matrix due to the presence of the colloidal particles. The range of the elastic forces is of the order of several colloidal diameters. Elastic forces drive the particles to self-assemble into linear chains,[7–10] periodic lattices,[10–12] anisotropic clusters,[13] and cellular structures.[14]

An additional distinctive feature of LC colloids is the presence of topological defects,[15] which determine the symmetry of the long-range colloidal interactions,[16,17] and are capable of stabilizing the ordered aggregates at short range,[2] where the elastic interactions are dominated by non-linear effects. Topological defects in nematic liquid crystals (NLC) are nucleated due to the mismatch of the global and local (at the colloidal surfaces) boundary conditions leading to frustration of the uniform nematic order. The complex dynamics of these defects renders the self-assembly of LC colloids a challenging theoretical problem.[18]

Small spherical particles ($\lesssim 1$ μm) imposing homeotropic surface anchoring on the nematic director stabilize equatorial Saturn-ring defects,[19] which for larger particles may be stabilized through confinement,[20] or by external electric fields.[21] The far-field distortions have quadrupolar symmetry and the resulting pairwise colloidal interaction is of the quadrupolar type decaying with the distance d between the particles as d^{-5}.[16]

Larger particles ($\gtrsim \mathcal{O}$ (1 μm)) with homeotropic anchoring induce point-like hedgehog defects,[22] which lead to a far-field director of dipolar symmetry and a large distance colloidal interaction varying as d^{-3}.[16] For particles with planar degenerate anchoring, two antipodal surface defects, known as boojums,[22] are nucleated which lead to a far-field director of quadrupolar symmetry. Recent numerical calculations revealed that the cores of nematic boojums can take three different configurations:[18] single core, double core, or split core. The single-core boojum is a point-like index 1 defect with azimuthal symmetry, the split-core

[a]*Centro de Física Teórica e Computacional, Universidade de Lisboa, Avenida Professor Gama Pinto 2, P-1649-003 Lisboa, Portugal*
[b]*Departamento de Física da Faculdade de Ciências, Universidade de Lisboa, Avenida Professor Gama Pinto 2, P-1649-003 Lisboa, Portugal. E-mail: nunos@cii.fc.ul.pt*
[c]*Department of Physics, Sharif University of Technology, P.O. Box: 11155-9161, Tehran, Iran*
[d]*Max-Planck-Institut für Intelligente Systeme, Heisenbergstr. 3, D-70569 Stuttgart, Germany. E-mail: miko@is.mpg.de*
[e]*Institut für Theoretische und Angewandte Physik, Universität Stuttgart, Pfaffenwaldring 57, D-70569 Stuttgart, Germany*

boojum has two index 1/2 surface point-like defects connected by a 1/2 bulk disclination line. The double-core boojum is an intermediated structure with broken azimuthal symmetry. The split core structure is favoured by low temperatures, strong anchoring and small twist to splay or bend ratios. For sufficiently strong anchoring potentials characterised by a well-defined uniaxial minimum, the split-core boojums are the only stable configuration.

For two interacting boojum-particles there are substantial rearrangements of the defects at short distances. These rearrangements of the defects are not only positional as reported in ref. 23 but also configurational. For example, for colloids oriented along the far-field director, $\theta = 0$ on Fig. 1, the inner single-core boojums undergo a configurational transition to split-core boojums, when the defect positions change, turning the $\theta = 0$ repulsion into an attraction. At shorter distances the split-core boojums on each colloid lock-in forming a double-bond defect structure between the particles, on the scale of the bulk correlation length, similar to that observed on the colloidal scale for spherical colloids in cholesterics.[24] The far-field distortions, however, and the resulting asymptotic pair interaction between particles with degenerate planar anchoring are of the quadrupolar type,[25] as for Saturn-ring particles.

Recently, a light sensitive coating of colloidal particles was used in order to switch the surface anchoring from homeotropic to planar, reversibly,[26] providing the means for tuning the colloidal interactions and thus controlling the assembly of the colloidal structures.

Direct assembly of two-dimensional (2D) crystallites of quadrupolar,[20] dipolar,[27] or dipolar and quadrupolar,[28] spherical particles has been achieved by using laser tweezer techniques. The crystallites are stabilized by the presence of topological defects, which provide local free energy minima of the order of $\sim$1000 k_BT, where k_B is the Boltzmann constant and T the absolute temperature. By contrast, interacting quadrupolar boojum-particles in three-dimensional systems do not exhibit short-range repulsive behaviour, on the colloidal scale, and the equilibrium configuration corresponds to close contact or coalescence of the particles.[18,23,29]

Recently, the assembly of 2D colloidal crystallites of spherical particles with two types of anchoring, homeotropic and degenerate planar, dispersed in 5CB has been reported.[30] The particles with radius $R = 2.16$ μm were confined to a cell of thickness 6 μm in order to stabilize the Saturn-ring configuration around the particles with homeotropic anchoring. Both types of particles generate quadrupolar nematic distortions, but the corresponding quadrupolar moments have different signs, meaning that the particles attract each other when they are aligned parallel or perpendicular to the far-field director. This allowed the assembly of 2D square colloidal crystallites. In the following we shall adopt the notation of ref. 30: a Saturn-ring quadrupolar particle will be denoted by "S", and a boojum quadrupolar particle by "P" (planar anchoring). In this article, we present the results of a numerical study of the NLC-mediated interaction between S and P particles (see Fig. 1) for a wide range of distances. We focus on the short-distance regime that determines the final equilibrium configuration and its stability. We use adaptive meshes to resolve the defect core configurations which were found to be crucial to determine the short-range equilibrium configurations accurately.

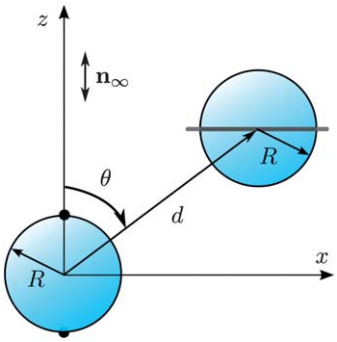

Fig. 1 Schematic representation of interacting Saturn-ring and boojum quadrupolar particles of radius R. d is the inter-particle distance and θ is the polar angle relative to the far-field director.

In contrast to the double-bond defect observed between P-particles, oriented along the far-field director, at short distances, the split core boojums and the Saturn ring, on P and S particles respectively, repel each other providing the mechanism for a short-range repulsion and an effective pair interaction with a well defined minimum.

The paper is organized as follows: in the next section we introduce the Landau-de Gennes free energy functional, which we minimize numerically. We give a very brief description of the numerical techniques that are described in detail in the Appendix of ref. 18. In Section 3 we present and discuss our results. We show that the S–P interaction exhibits two local minima for configurations where the particles align either parallel or perpendicular to the far-field director, thus allowing the assembly of square lattices. We also show that the two equilibrium configurations are separated by a free energy barrier of the order of 250 $k_BT(R/1\ \mu m)$, where R is the colloidal radius. A comparison with the experimental results reported in ref. 30 reveals that the accuracy of the theoretical description is excellent. In Section 4 we present our conclusions and discuss perspectives for further work. In particular we point out that the effects of polydispersity and of the anchoring strength may hinder/promote the relative stability of the two orthogonal minima required for the assembly of square crystallites and may have to be taken into account, in more general terms.

2 Landau-de Gennes theory

Phenomenologically, nematic liquid crystals are characterised by a traceless, symmetric tensor order-parameter $\boldsymbol{Q}$ which can, in general, be written as[31]

$$Q_{ij} = \frac{Q}{2}\left(3n_in_j - \delta_{ij}\right) + \frac{B}{2}\left(l_il_j - m_im_j\right), \quad (1)$$

where Q is the uniaxial order parameter, which measures the degree of orientational order along the nematic director $\boldsymbol{n}$, and B is the biaxial order parameter, which measures the degree of orientational order along the directions perpendicular to $\boldsymbol{n}$, characterised by $\boldsymbol{l}$ and $\boldsymbol{m}$. The corresponding Landau-de Gennes (LdG) free energy functional is[32]

$$F = \int_{\Omega} \mathrm{d}^3x(f_b + f_e) + \int_{\partial\Omega} \mathrm{d}s f_s, \quad (2)$$

where f_b and f_e are the bulk and elastic free energy densities, given by

$$f_b = a(T)\mathrm{Tr}\boldsymbol{Q}^2 - b\mathrm{Tr}\boldsymbol{Q}^3 + c(\mathrm{Tr}\boldsymbol{Q}^2)^2 \quad (3)$$

$$f_e = \frac{L}{2}(\partial_k Q_{ij})^2. \quad (4)$$

The first integral in eqn (2) is over the volume occupied by the nematic, Ω, and the second is over the surfaces of the colloidal particles, $\partial\Omega$. The bulk parameter $a(T) = a_0(T - T^*)$ depends linearly on the temperature T, with a_0 being a material dependent constant and T^* the supercooling temperature of the isotropic phase; b and c are positive material dependent constants. For a given temperature T and in the absence of elastic distortions the free energy density in eqn (3) is minimized for the (bulk) degree of orientational order given by

$$Q_b = \frac{b}{8c}\left(1 + \sqrt{1 - \frac{8\tau}{9}}\right), \quad (5)$$

where $\tau = 24a_0(T - T^*)c/b^2$ is the reduced temperature. τ controls the stability of the nematic and isotropic phases. For $\tau > 9/8$ the nematic phase is unstable, while the isotropic phase is unstable for $\tau < 0$. The nematic and the isotropic phases coexist at $\tau = 1$. For simplicity, we consider the one-elastic constant approximation where L is related to the Frank–Oseen (FO) elastic constant K by $K = 9Q^2L/2$.[31]

We consider the interaction between colloidal particles with homeotropic and degenerate planar anchoring. We assume rigid homeotropic boundary conditions, while the planar degenerate anchoring is described by the covariant surface anchoring free energy proposed by Fournier and Galatola (FG):

$$f_s = W_1(\tilde{Q}_{ij} - \tilde{Q}_{ij}^{\perp})^2 + W_2(\tilde{Q}_{ij}^2 - (3Q_b/2)^2)^2, \quad (6)$$

$\tilde{Q}_{ij} = Q_{ij} + Q_b\frac{\delta_{ij}}{2}$, $\tilde{Q}_{ij}^{\perp} = (\delta_{ik} - \nu_i\nu_k)\tilde{Q}_{kl}(\delta_{lj} - \nu_l\nu_j)$, and ν is the surface normal. The quadratic term favours tangential orientation of the director $\boldsymbol{n}$, and the quartic term guarantees the existence of a minimum for the scalar order parameter at the surface equal to its bulk value Q_b. For simplicity we will assume $W_1 = W_2 = W$. Under these conditions the boojums nucleated at the colloidal surface have split cores, *i.e.*, the boojum has two index 1/2 surface point-like defects connected by a 1/2 bulk disclination line.[18] The equilibrium surface orientation is determined by the free energy functional minimum that satisfies the far-field $\boldsymbol{n}_\infty$ boundary conditions.

Typical values of bulk parameters for 5CB are $a_0 = 0.044 \times 10^6$ J K^{-1} m^{-3}, $b = 0.816 \times 10^6$ J m^{-3}, $c = 0.45 \times 10^6$ J m^{-3}, $L = 6 \times 10^{-12}$ J m^{-1}, and $T^* = 307$ K. At the nematic–isotropic coexistence the bulk correlation length $\xi = (24\,cL/b^2)^{1/2} \simeq 10$nm determines the order of magnitude of the spatial extension of the cores of the topological defects.[33] Calculations were performed for particles of radius $R = 0.1\,\mu\mathrm{m} \simeq 10\xi$, in a cubic box of length $l = 30R$; the reduced temperature $\tau \simeq 0.16$, and the anchoring strength W satisfies $WQ_b^2R/K \simeq 37$, corresponding to the strong anchoring regime. In this regime P-particles nucleate a pair of split-core boojums of the order of the bulk correlation length.[18] The short-range interaction of the split-core boojums on P-particles with the Saturn-rings nucleated around the equatorial plane of the S-particles will be investigated in what follows. We find that the defects are re-arranged but they repel each other, along the $\theta = 0$ and the $\theta = \pi/2$ directions which are attractive at large distances, providing the mechanism for the short-range repulsion that prevents the particles from coalescing.

The Landau-de Gennes free energy eqn (2) is minimized using finite element methods, with adaptive meshing. The adaptive meshing is crucial to describe the structure of the defect cores and to calculate the short-range interactions accurately. The surfaces of the spherical particles $\partial\Omega$ are triangulated using the open source *GNU Triangulated Surface Library*.[34] Then, the triangulation of the nematic domain Ω is carried out using the *Quality Tetrahedral Mesh Generator*,[35] which supports adaptive mesh refinement. Linear triangular and tetrahedral elements are used in 2D and 3D, respectively. Generalized Gaussian quadrature rules for multiple integrals[36] are used in order to evaluate the integrals over the elements. In particular, for tetrahedra a fully symmetric cubature rule with 11 points[37] is used, and integrations over triangles are done using a fully symmetric quadrature rule with 7 points.[38] The discretized Landau-de Gennes functional is then minimized using the *INRIA*'s *M1QN3* (ref. 39) optimization routine, which implements a limited memory quasi-Newton technique reported by Nocedal.[40] More details may be found in the Appendix of ref. 18.

3 Results

We consider the far-field director $\boldsymbol{n}_\infty$ parallel to the z-axis, and place an S or a P particle at the origin of the reference frame. For spherical particles, the distortions of the director field $\boldsymbol{n}(\boldsymbol{r})$ are uniaxial, with the symmetry group $C_{\infty v}$. At large distances r from the particle, the director exhibits small distortions from its uniform far-field alignment $\boldsymbol{n}(\boldsymbol{r}) \simeq (n_1, n_2, 1 - \mathcal{O}(n_1^2, n_2^2))$. In the one-elastic constant approximation, the transverse components $n_i (i = 1, 2)$ satisfy Laplace's equation $\Delta n_i = 0$,[25] and the asymptotic solution for n_i can be expanded in terms of multipoles. Due to the symmetry requirements, the quadrupolar term is the lowest-order term in the expansions,[25] *i.e.*,

$$n_i = 5\sum_{\alpha,\beta=1}^{3} Q_{i\alpha\beta}\frac{r_\alpha r_\beta}{r^5} + \ldots, \quad (7)$$

and the symmetry of the director requires the quadrupole moment tensor $Q_{i\alpha\beta} = Q\delta_{i\alpha}\delta_{3\beta}$. In ref. 25 an explicit expression for $Q_{i\alpha\beta}$ in terms of surface integrals involving n_i is given. Applying the superposition approximation, the pair interaction between quadrupolar particles is obtained,[25,41]

$$F_{1Q-1Q} = \frac{80\pi K}{9d^5}Q_1Q_2(9 - 90\cos^2\theta + 105\cos^4\theta), \quad (8)$$

where the subscript indicates that the interaction is between two uniaxial quadrupoles with moments Q_1 and Q_2. For $Q_1 = Q_2$, the interaction in eqn (8) is repulsive at $\theta = 0$ and $\theta = \pi/2$, and attractive at intermediate orientations. The effective interactions between two S or two P particles have been analysed theoretically beyond the superposition approximation in ref. 6,18 and 23. In both cases, significant deviations from the asymptotic quadrupolar behaviour have been found at short distances.

The interaction between S and P particles was measured recently.[30] An asymptotic analysis suggests that S particles

induce elastic quadrupoles with quadrupole moments $Q_S > 0$. In contrast, P particles are characterised by quadrupole moments $Q_P < 0$.[25] The sign of a quadrupole moment cannot be obtained from the interaction between like quadrupoles, S–S or P–P; only the absolute value may be extracted from such experiments. Different experiments yield a range of values, summarised in Table 1. The discrepancies are most likely due to the different conditions (*e.g.*, geometrical confinement) under which the experiments were carried out,[42] or to the effects of thermal fluctuations that are important at large distances.[29] These factors may limit (severely) the range of validity of the asymptotic expression, eqn (8).

Recent numerical calculations reveal that under certain conditions the boojums of P particles have a split core structure with broken axial symmetry.[18] In this case, the P particle induces a biaxial quadrupole[25] adding a correction to the asymptotic result, eqn (8). However, since the core size is of the order of the nematic correlation length, the effects of the biaxiality are small far away from the particle. Indeed, as we shall demonstrate below, our calculations are in good agreement with eqn (8) indicating that the biaxial contribution is unimportant.

We calculate the two-body effective interaction $F^{(2)}(d,\theta)$,[44] defined by decomposing the excess (over the bulk) free energy for two particles $F_2 \equiv F - f_b(Q_b)\Omega$ as

$$F_2(d,\theta) = F_S^{(1)} + F_P^{(1)} + F^{(2)}(d,\theta) \quad (9)$$

where $F_{S,P}^{(1)}$ is the excess free energy of an isolated S or P particle, respectively. By definition, $F^{(2)}$ tends to zero when $d \to \infty$.

Fig. 2 illustrates the S–P interaction $F^{(2)}(d)$ for several values of θ. In contrast to the S–S and P–P interactions, the S–P interaction is purely attractive at $\theta = 0$, $\pi/2$, and repulsive at intermediate orientations, which is consistent with $Q_S Q_P < 0$. As shown in Fig. 2, the asymptotic result, eqn (8), is accurate for $d \gtrsim 3R$. For smaller distances the superposition approximation is qualitatively wrong, indicating the significance of non-linear effects. $F^{(2)}(d,\theta)$ exhibits a local minimum at $d_\perp \simeq 2.25R$, corresponding to $\theta = \pi/2$, and a global minimum at $d_\parallel \simeq 2.16R$ for relative orientation $\theta = 0$ (see also Fig. 4). These values are in excellent agreement with the experimental results $d_\perp^{exp} \simeq 2.28R$ and $d_\parallel^{exp} \simeq 2.16R$.[30] At $\theta = \pi/4$, $F^{(2)}(d)$ reveals a crossover from repulsive behaviour, at large $d \gtrsim 2.9R$, to attractive behaviour, at smaller $d \lesssim 2.9R$. The crossover is driven by the structural re-arrangement of the defects (see the configurations in Fig. 4a and b). This is similar to the crossover observed in the S–S interaction[6] at $\theta = \pi/2$, where the Saturn-rings deform from their equatorial position, or for the P–P interaction at $\theta = 0$, where the inner boojums slide on the colloidal surfaces in opposite directions.[18,23] In the S–P interaction, however, we observe both the sliding of the inner boojum and the deformation of the Saturn-ring, as shown in Fig. 4. The configuration at $\theta = \pi/4, d \simeq 2.14R$ does not correspond to a local minimum of the S–P interaction. In fact, $F^{(2)}(d, \theta)$ in the vicinity of that point has a cusp-like shape in the θ-direction (see Fig. 4). At very small distances, however, the conflicting anchoring conditions on the particle surfaces lead to a repulsive $F^{(2)}(d)$ at any orientation θ.

Table 1 Absolute values of the elastic quadrupole moment $|Q_P|$ reported by different experiments for spherical colloidal particles with planar degenerate anchoring

Cell thickness (μm)	$2R$ (μm)	$\lvert Q_P\rvert$ (R^3)	Ref.
8	4.5	0.17	43
6.5–8	4	0.2	42
6	4.32	0.5	30
30–100	3–7.5	0.66	29

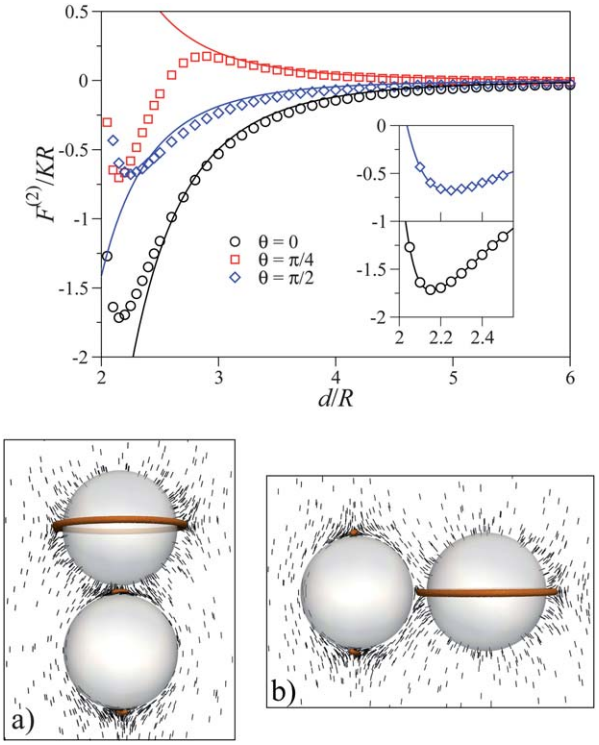

Fig. 2 Pair interaction $F^{(2)}$ as a function of inter-particle separation d for different orientations $\theta = 0$, $\pi/4$, $\pi/2$, relative to the far-field director (see Fig. 1). Coloured lines represent the asymptotic result, eqn (8), with $Q_S Q_P = -0.18R^6$. The inset shows in more detail the global ($\theta = 0$) and local ($\theta = \pi/2$) minima located at $d = d_\parallel \simeq 2.16R$ and $d = d_\perp \simeq 2.25R$, respectively. The nematic configurations are illustrated in (a) for the global minimum at $\theta = 0$, $d = d_\parallel$, and in (b) for the local minimum at $\theta = \pi/2$, $d = d_\perp$. The iso-surfaces correspond to $Q = 0.25$, $Q_b \simeq 0.44$, and the short black lines represent the director field in the plane $y = 0$.

This can be seen also from the behaviour of the elastic force $\mathbf{F}(d,\theta)$ between the colloidal particles. Fig. 3 shows the radial $F_r = -\partial F^{(2)}/\partial d$ and the polar $F_\theta = -(1/d)\partial F^{(2)}/\partial\theta$ components of the force as functions of d for several values of θ. It is clear that for the orientations $\theta = 0$ and $\theta = \pi/2$ the interaction is purely attractive at large separations d, and that a strong repulsion appears at very small d, in all directions, stabilizing the dimer at a fixed separation $d > 2R$. Moreover, the behaviour of F_θ clearly shows that once the particles are oriented along $\theta = 0$ or $\theta = \pi/2$ they will approach each other along this direction under the action of F_r, and will stabilize at $d = d_\parallel$ or $d = d_\perp$, respectively. The radial component of the force at $\theta = \pi/4$ is repulsive for large inter-particle distances, and turns into attractive as soon as the defects start to rearrange. Although the asymptotic result, eqn (8), predicts a non-zero $F_\theta < 0$ at $\theta = \pi/4$, *i.e.*, a polar component of the force which tends to align the particles parallel to $\boldsymbol{n}_\infty$, it is

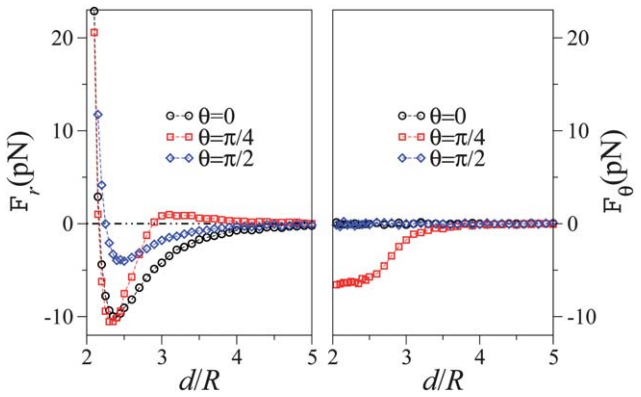

Fig. 3 Radial F_r and polar F_θ components of the force acting on the colloidal particles as a function of the inter-particle distance d, for several orientations $\theta = 0$, $\pi/4$, $\pi/2$, relative to the far-field director $\boldsymbol{n}_\infty$.

only when the non-linear elastic effects become important ($d \lesssim 3R$) that F_θ increases significantly and becomes comparable to F_r. This is in sharp contrast to the P–P interaction force,[18] where F_θ is always two orders of magnitude smaller than F_r.

Fig. 4 illustrates the interaction $F^{(2)}(\theta)$ for several values of the inter-particle distance d. At $d = 3.0R$ the interaction is a smooth function of θ. It is clear that for this distance the asymptotic result, eqn (8), represented in Fig. 4 using the experimental value $Q_S Q_P = -0.18R^6$, is qualitatively but not quantitatively accurate. As mentioned previously, the asymptotic result describes the full LdG results quantitatively at distances $d > 3R$. As the distance between the particles decreases, $F^{(2)}(\theta)$ reveals a cusp at some oblique angle θ. This corresponds to a structural transition between two different nematic configurations, which "coexist" at the orientation corresponding to the cusp. Two representative nematic configurations are shown at $d = 2.4R$ in Fig. 4a at $\theta \simeq 0.55(\pi/2)$ and in Fig. 4b at $\theta \simeq 0.62(\pi/2)$. When the S and P colloidal particles are at the equilibrium configuration at $\theta = 0$, an increase in θ forces the inner boojum to slide in the same direction as a result of the repulsion from the disclination ring, which deforms upwards from its equatorial position, as depicted in Fig. 4a. The S–P system follows the left branch of $F^{(2)}(\theta)$ as θ increases from zero. This configuration becomes metastable at the cusp and at a larger value of $\theta^*(d)$ the repulsion between the inner boojum and the disclination ring renders it unstable. Then, the system jumps to the right branch, and assumes a configuration similar to that depicted in Fig. 4b. On the other hand, when the S–P system starts from the local equilibrium configuration at $\theta = \pi/2$, it follows the right branch of $F^{(2)}$ as θ decreases. The disclination ring now deforms downwards and pushes one of the boojums away from the z-axis as depicted in Fig. 4b.

An overview of the pair interaction $F^{(2)}$ as a function of the inter-particle distance d and the orientation with respect to the far-field director θ is illustrated in Fig. 5 where we combine the results plotted in Fig. 2 and 4. The minima at short distances is clearly visible for particles aligned parallel ($\theta = 0$) or perpendicular ($\theta = \pi/2$) to the far-field director. The barrier between these configurations, at fixed separation, is smooth at large distances and becomes sharp at short distances, signalling the structural transition that drives the re-orientation of the defects. The existence of two minima at $\theta = 0$, $\pi/2$, with long distance

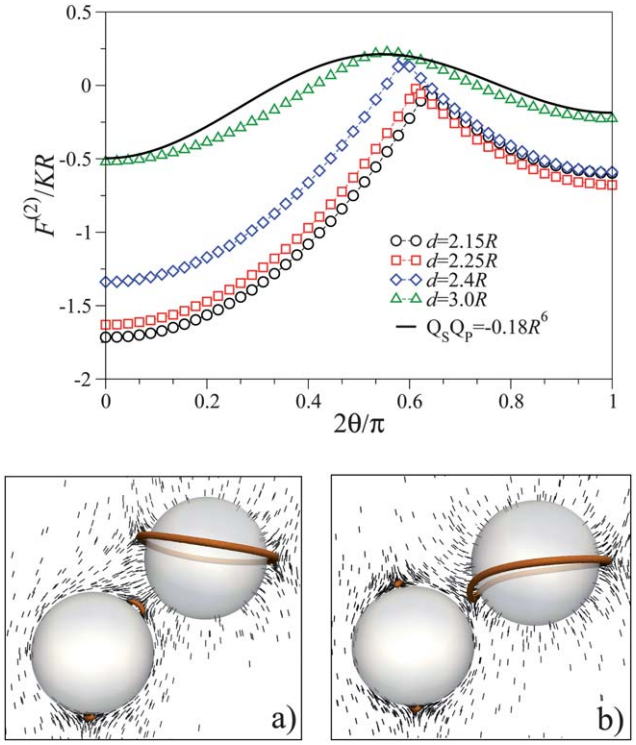

Fig. 4 Pair interaction $F^{(2)}$ as a function of the relative orientation θ for different inter-particle distances d. The black line shows the asymptotic result, eqn (8), with $Q_S Q_P = -0.18R^6$ at $d = 3R$. The snapshots depict the nematic configurations obtained from the numerical calculations at $d = 2.4R$: (a) $\theta \simeq 0.55(\pi/2)$ and (b) $\theta \simeq 0.62(\pi/2)$ close to the free-energy cusp. The isosurfaces correspond to $Q = 0.25$ and $Q_b \simeq 0.44$, and the short black lines represent the director field in the plane $y = 0$.

attraction, is a new feature that has not been observed in either S–S or P–P interactions. In the case of two interacting S particles, the pair interaction potential exhibits a single minimum at an oblique angle $\theta \simeq 0.62(\pi/2)$ with the far-field director,[2] which enables the assembly of colloidal crystals with rhombic unit cell. The pair interactions of P particles do not exhibit a short-range repulsion in any direction, and particles usually bundle at an oblique angle $\theta \simeq 0.33(\pi/2)$.[23,29] Recent numeric calculations suggest that, under some conditions, the P–P interaction free

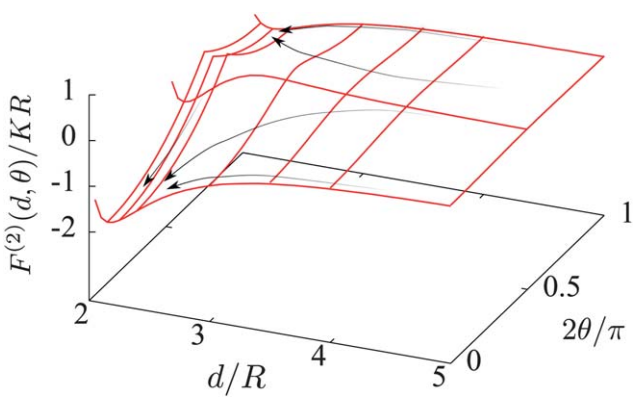

Fig. 5 Pair interaction $F^{(2)}$ as a function of the inter-particle distance d and the orientation θ. The sketched arrows indicate possible trajectories towards the equilibrium configurations.

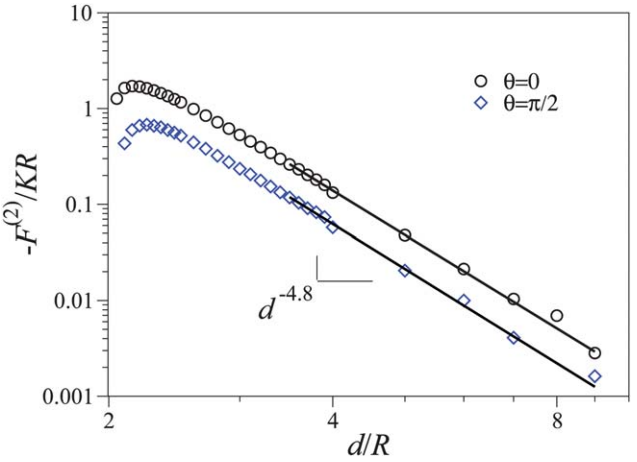

Fig. 6 Pair interaction $F^{(2)}$ as a function of the inter-particle distance d for $\theta = 0, \pi/2$. Black lines correspond to a power law fit $F^{(2)} = f(\theta)(R/d)^{\alpha(\theta)}$ to the numerical results. In both cases $\alpha = 4.8 \pm 0.2$.

energy can have an additional minimum at $\theta = 0$ related to a structural change and the sharing of the inner surface defects,[18] leading to the formation of chains aligned with the far-field director, similar to what was found in cholesterics.[24] However, in this case the assembly would have to be induced to overcome the long-distance repulsion along this direction.

It is clear from Fig. 2 and 4, that at short-distances $d \lesssim 3R$ the inter-particle interaction deviates significantly from the asymptotic result described by eqn (8). In Fig. 6 we plot the absolute value of the S–P interaction as a function of d for $\theta = 0, \pi/2$. For large separations, $d \gtrsim 3R$, $F^{(2)}(d)$ is described by a power law

$$F^{(2)} = f(\theta)(R/d)^{\alpha(\theta)} \quad (10)$$

where both $\alpha(\theta)$ and $f(\theta)$ are fitting parameters. Fig. 2 indicates that the asymptotic result is valid for $d \gtrsim 3R$. Thus, in Fig. 6 we fit eqn (10) to the results corresponding to $d \geq 3.5R$ only. For both values of θ we find $\alpha = 4.8 \pm 0.2$, which is in line with the asymptotic power law $\propto 1/d^5$. From these fits we also obtain $Q_S Q_P/R^6 = -0.15 \pm 0.03$ and $Q_S Q_P/R^6 = -0.20 \pm 0.05$ for $\theta = 0$ and $\theta = \pi/2$, respectively, in excellent agreement with the experimental value $Q_S Q_P/R^6 = -0.18$ reported in ref. 30.

4 Conclusions

Recently, a directed assembly of spherical particles, dispersed in a nematic host, into 2D square crystal-like structures was reported.[30] This was achieved by mixing quadrupolar colloidal particles with distinct anchoring conditions, namely homeotropic and degenerate planar. The homeotropic anchoring particles nucleate Saturn-ring defects, and the planar anchoring particles antipodal boojums. In the linear regime each of these colloidal particles induce long-range distortions of the nematic director with quadrupolar symmetry,[45] and as a result the long-range pair interaction is of the quadrupolar type. In this paper we have studied numerically the nematic-mediated interaction between two such particles. For simplicity we have assumed spherical particles of equal radii and set the surface fields well in the strong anchoring regime, where the non-linear effects that set in at short-distances are strongest.

We have confirmed that the S and P particles have quadrupole moments with opposite signs, $Q_S Q_P < 0$. The asymptotic analysis[25] suggests that S particles have a positive quadrupole moment, and P particles a negative one. At large distances the interaction $F^{(2)}(d, \theta)$ behaves as $d^{-\alpha}$ with $\alpha = 4.8 \pm 0.2$ which is in excellent agreement with the asymptotic result d^{-5} for quadrupolar interactions. We have also confirmed numerically the experimental values for the product of the quadrupole moments $Q_S Q_P = -0.18R^6$. Note that if the confining surfaces of the experimental cell[30] had an influence on the pair interaction, there would be a deviation from the power law behaviour that would eventually (for strong confinement) turn into an exponential decay. As in our calculations finite size effects are practically absent, and the agreement with the experimental results[30] indicates that the effect of the confining cell surfaces is negligible. For distances $d \lesssim 3R$, the asymptotic quadrupolar result, eqn (8), is qualitatively wrong; see Fig. 2. At such distances the topological defects start to interact and re-arrange their positions (see Fig. 4a and b), resulting in profound changes of the interaction $F^{(2)}(d)$ (see Fig. 2, red squares).

The P particles considered here nucleate boojums with complex biaxial structures.[18] This leads to a biaxial quadrupolar distortion, breaking the axial symmetry, and could change the asymptotic uniaxial field given by eqn (8).[25] However, the size of the biaxial regions is of the order of the nematic correlation length, and the biaxial perturbation at large distances is negligible, as shown by the agreement between our numerical results and the asymptotic uniaxial quadrupolar field.

In contrast to the interaction of particles with identical anchoring conditions (P–P or S–S), the S–P interaction $F^{(2)}(d,\theta)$ exhibits two minima (in the first quadrant), for particles oriented at $\theta = 0$ and $\theta = \pi/2$ relative to the far-field director, and separated by $d_{\parallel} \simeq 2.16R$ and $d_{\perp} \simeq 2.25R$, respectively; see Fig. 2. These values are in excellent agreement with those reported experimentally,[30] $d_{\parallel}^{exp} \simeq 2.16R$ and $d_{\perp}^{exp} \simeq 2.28R$.[30] We also found a strong repulsion at short distances at any orientation θ. These two features of the pair interaction are pre-requisites for the assembly of colloidal lattices with rectangular unit cells.

We found that the polar component of the elastic force F_θ is always zero at $\theta = 0, \pi/2$, and increases considerably at oblique orientations, for inter-particle distances which are not too large ($d \lesssim 3R$, see Fig. 3 right panel). The sign of F_θ depends on θ. $F_\theta < 0$ for $\theta \leq \theta^c(d)$, and it is positive otherwise. $\theta^c(d)$ is the angular position of the cusp in the $F^{(2)}(\theta)$ profile; see Fig. 4. Therefore, there is a strong elastic force which aligns a pair of colloidal particles either parallel ($\theta \leq \theta^c(d)$) or perpendicular ($\theta \geq \theta^c(d)$) to the far-field director. Once the particles are aligned along one of these directions, they move under the action of the radial force F_r towards the global $d = d_{\parallel}$, $\theta = 0$, or the local $d = d_{\perp}$, $\theta = \pi/2$ equilibrium positions. The presence of a strong aligning force F_θ at small-to-intermediate distances is in sharp contrast to the P–P interaction profile,[18] where the polar component F_θ is always two orders of magnitudes smaller than the radial force F_r.

As in most theoretical studies of interactions between colloidal particles in nematic liquid crystals, our study considers particles with the same size. This is a rather strong simplification justified, in part, by the current experimental ability to produce

monodispersed colloidal particles. Although this seems to be a good choice for the assembly of photonic crystals, the effect of polydispersity on the stability of the crystals may hold surprises and remains an important open question that will be addressed in the future. Likewise, the choice of surface fields (rigid homeotropic and uniaxial planar in the strong anchoring regime) is an additional tuning parameter that will have an effect on the stability of the crystal. The well defined minima at short-range for both orientations and the large free energy barrier between them suggest that this choice is not critical, as long as we remain in the strong anchoring regime.

Note added after first publication

This article replaces the version published on 20th August 2012, which contained errors in eqn (1), (4), (5), (7) and (8), and in the text below eqn (6).

Acknowledgements

We gratefully acknowledge financial support from the Portuguese Foundation for Science and Technology (FCT) through grants no. PEstOE/FIS/U10618/2011, PTDC/FIS/098254/2008, and SFRH/BPD/40327/2007 (NMS). We also acknowledge partial financial support from FCT-DAAD Transnational Cooperation Scheme under the grant no. 50108964, and the FP7 IRSES Marie-Curie grant PIRSES-GA-2010-269181.

References

1 I. Muševič, M. Škarabot and M. Humar, *J. Phys.: Condens. Matter*, 2011, **23**, 284112.
2 I. Muševič, M. Škarabot, U. Tkalec, M. Ravnik and S. Žumer, *Science*, 2006, **313**, 954.
3 M. Ravnik, M. Škarabot, S. Žumer, U. Tkalec, I. Poberaj, D. Babič, N. Osterman and I. Muševič, *Phys. Rev. Lett.*, 2007, **99**, 247801.
4 D. Kang, J. Maclennan, N. Clark, A. Zakhidiv and R. Baughman, *Phys. Rev. Lett.*, 2001, **86**, 4052.
5 H. Stark, *Phys. Rep.*, 2001, **351**, 387–474.
6 M. Tasinkevych and D. Andrienko, *Condens. Matter Phys.*, 2010, **13**, 33603.
7 J.-C. Loudet, P. Barois and P. Poulin, *Nature*, 2000, **407**, 611.
8 P. Cluzeau, P. Poulin, G. Joly and H. Nguyen, *Phys. Rev. E: Stat., Nonlinear, Soft Matter Phys.*, 2001, **63**, 031702.
9 P. Cluzeau, G. Joly, H. Nguyen and V. Dolganov, *JETP Lett.*, 2002, **75**, 482.
10 C. Völtz and R. Stannarius, *Phys. Rev. E: Stat., Nonlinear, Soft Matter Phys.*, 2004, **70**, 061702.
11 V. G. Nazarenko, A. Nych and B. Lev, *Phys. Rev. E: Stat., Nonlinear, Soft Matter Phys.*, 2001, **87**, 075504.
12 P. Cluzeau, G. Joly, H. T. Nguyen and V. K. Dolganov, *JETP Lett.*, 2002, **75**, 482.
13 P. Poulin, N. Frances and O. Mondail-Monval, *Phys. Rev. E: Stat. Phys., Plasmas, Fluids, Relat. Interdiscip. Top.*, 1999, **59**, 4384.
14 S. P. Meeker, W. P. J. Crain and E. Terentjev, *Phys. Rev. E: Stat. Phys., Plasmas, Fluids, Relat. Interdiscip. Top.*, 2000, **61**, R6083.
15 N. D. Mermin, *Rev. Mod. Phys.*, 1979, **51**, 591–648.
16 T. C. Lubensky, D. Pettey, N. Currier and H. Stark, *Phys. Rev. E: Stat. Phys., Plasmas, Fluids, Relat. Interdiscip. Top.*, 1998, **57**, 610.
17 B. I. Lev and P. M. Tomchuk, *Phys. Rev. E: Stat. Phys., Plasmas, Fluids, Relat. Interdiscip. Top.*, 1999, **59**, 591.
18 M. Tasinkevych, N. M. Silvestre and M. M. Telo da Gama, *New J. Phys.*, 2012, **14**, 073030.
19 Y. D. Gu and N. L. Abbott, *Phys. Rev. Lett.*, 2000, **85**, 4719.
20 M. Škarabot, M. Ravnik, S. Žumer, U. Tkalec, I. Poberaj, D. Babič, N. Osterman and I. Muševič, *Phys. Rev. E: Stat., Nonlinear, Soft Matter Phys.*, 2008, **77**, 031705.
21 J. Loudet and P. Poulin, *Phys. Rev. Lett.*, 2001, **87**, 165503.
22 P. Poulin and D. Weitz, *Phys. Rev. E: Stat. Phys., Plasmas, Fluids, Relat. Interdiscip. Top.*, 1998, **57**, 626.
23 M. R. Mozaffari, M. Babadi, J. Fukuda and M. R. Ejtehadi, *Soft Matter*, 2011, **7**, 1107–1113.
24 F. E. Mackay and C. Denniston, *EPL*, 2011, **94**, 66003.
25 V. M. Pergamenshchik and V. A. Uzunova, *Condens. Matter Phys.*, 2010, **13**, 33602.
26 S. Chandran, F. Mondiot, O. Mondain-Monval and J. C. Loudet, *Langmuir*, 2011, **27**, 15185.
27 M. Škarabot, M. Ravnik, S. Žumer, U. Tkalec, I. Poberaj, D. Babič, N. Osterman and I. Muševič, *Phys. Rev. E: Stat., Nonlinear, Soft Matter Phys.*, 2007, **76**, 051406.
28 U. Ognysta, A. Nych, V. Nazarenko, M. Škarabot and I. Muševič, *Langmuir*, 2009, **25**, 12092.
29 I. I. Smalyukh, O. D. Lavrentovich, A. N. Kuzmin, A. V. Kachynski and P. N. Prasad, *Phys. Rev. Lett.*, 2005, **95**, 157801.
30 U. M. Ognysta, A. B. Nych, V. A. Uzunova, V. M. Pergamenshchik, V. G. Nazarenko, M. Skarabot and I. Musevic, *Phys. Rev. E: Stat., Nonlinear, Soft Matter Phys.*, 2011, **83**, 041709.
31 M. C. J. M. Vissenberg, S. Stallinga and G. Vertogen, *Phys. Rev. E: Stat. Phys., Plasmas, Fluids, Relat. Interdiscip. Top.*, 1997, **55**, 4367–4377.
32 P. G. de Gennes and J. Prost, *The Physics of Liquid Crystals*, Clarendon, Oxford, 2nd edn, 1993.
33 S. Chandrasekhar, *Liquid Crystals*, Cambridge University, 2nd edn, 1992.
34 GNU Triangulated Surface Library, 2006, http://gts.sourceforge.net.
35 H. Si, TetGen. A Quality Tetrahedral Mesh Generator and a 3D Delaunay Triangulator, 2011, http://wias-berlin.de/software/tetgen/.
36 R. Cools, *J. Complex.*, 2003, **19**, 445–453.
37 P. Keast, *Comput. Methods Appl. Mech. Eng.*, 1986, **55**, 339–348.
38 A. H. Stroud, *Approximate Calculation of Multiple Integrals*, Prentice-Hall, Englewood Cliffs, N.J., 1971.
39 J. C. Gilbert and C. Lemaréchal, *Math. Program.*, 1989, **45**, 407–435.
40 J. Nocedal, *Math. Comput.*, 1980, **35**, 773.
41 V. Pergamenshchik and V. Uzunova, *Eur. Phys. J. E*, 2007, **23**, 161.
42 M. Vilfan, N. Osterman, M. Čopič, M. Ravnik, S. Žumer, J. Kotar, D. Babič and I. Poberaj, *Phys. Rev. Lett.*, 2008, **101**, 237801.
43 J. Kotar, M. Vilfan, N. Osterman, D. Babič, M. Čopič and I. Poberaj, *Phys. Rev. Lett.*, 2006, **96**, 207801.
44 M. Tasinkevych and D. Andrienko, *Eur. Phys. J. E*, 2006, **21**, 277–282.
45 B. I. Lev, S. B. Chernishuk, P. M. Tomchuk and H. Yokoyama, *Phys. Rev. E: Stat., Nonlinear, Soft Matter Phys.*, 2002, **65**, 021709.

